Massive Star Birth: A Crossroads of Astrophysics
Proceedings IAU Symposium No. 227, 2005
R. Cesaroni, M. Felli, E. Churchwell & C. M. Walmsley, eds.

doi:10.1017/S1743921305004618

X-ray studies of massive star birth regions

Katsuji Koyama
Department of Physics, Kyoto University
email: koyama@cr.scphys.kyoto-u.ac.jp

Abstract. I report X-ray features of young stage of intermediate and high mass stars. The giant molecular cloud Sagittarius B2 (Sgr B2) exhibits more than dozen X-ray sources, two are associated with the ultra compact (UC) HII complex, Sgr B2 Main. The sources show large absorption of $\gg 10^{23}$ Hcm^{-2}, the largest among any known stellar X-ray sources.

The Arches cluster exhibits 3 extremely bright (a few $\times 10^{33}$ ergs s^{-1}) X-ray sources associated with the infrared (IR) massive stars. The X-ray spectra have 1-3 keV temperature in thin thermal model. Elongated diffuse 6.4 keV line emission is found.

The Monoceros R2 cloud exhibits half dozen X-ray sources associated with young high-mass IR stars. They show rapid time variability and a thin thermal spectrum of $\sim$2 keV temperature.

Among 28 *ASCA* pointing on intermediate-mass pre-main-sequence stars, or Herbig Ae/Be stars (HAeBes), eleven are found to be plausible X-ray sources. The general X-ray properties of these HAeBes are; (1) the plasma temperature and time variability are higher than those of high mass main-sequence stars, and more similar to low mass stars; (2) the X-ray luminosities come to the upper end of low mass pre-main sequence stars, or in some cases exceed that; (3) the X-ray activity of HAeBe decreases at the age of about a few$\times 10^6$ years.

Using above observational facts, I propose a unified picture of X-ray activity of young stars in the wide mass range.

Keywords. radiation mechanisms, massive young stars, evolution, magnetic fields, pre-main sequence, X-rays

1. Introduction

Since high mass stars evolve very rapid, and are generally located at long distance, the X-ray observations and samples of high mass young stellar objects (YSOs) are largely limited. Therefore the X-ray study is fur behind low mass stars.

The *ASCA* satellite has found hard X-rays from the center of giant molecular clouds (GMCs), the site of high mass star formation. *ASCA* also pointed many intermediate mass young stars (HAeBes). Since the limited spatial resolution of *ASCA* did not allow us to uniquely resolve high mass YSOs in the GMCs, we performed follow-up observations with *Chandra*.

This report is based on the *ASCA* and recent *Chandra* results. The star forming regions referred in this paper are: Sagittarius B2 (Sgr B2), Arches Cluster, Monoceros R2 (Mon R2), and many Herbig Ae/Be stars (HAeBes). Details of individual sources are given in Takagi, Murakami & Koyama (2002), Kohno, Koyama & Hamaguchi (2002) and Hamaguchi, Yamauchi & Koyama (2005).

2. High Mass Star Forming Regions

2.1. *The Sgr B2 cloud*

Sgr B2 is a giant molecular cloud located at a projected distance of 100 pc from the Galactic center (GC). Due to its proximity to the GC and its high density cores, high mass YSOs, possibly in the cores are heavily obscured in the optical, even near infrared (NIR) and soft X-ray bands. Therefore the study of star formation activity has been limited to the radio or fur infrared (FIR)

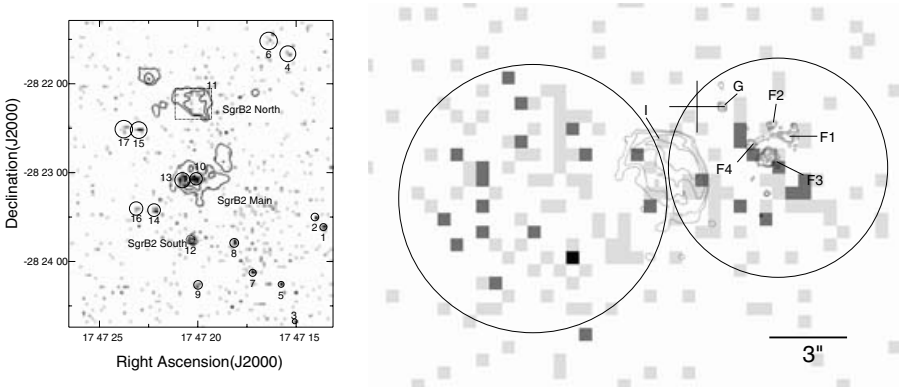

Figure 1. Left: The X-ray image of Sgr B2 overlaid on the HII complex. Right: The closed-up view near the ultra compact HII complex, Sgr B2 Main. The X-ray bin size is $0.5'' \times 0.5''$. [adopted from Takagi, Murakami & Koyama (2002)]

bands. The radio continuum bands have revealed nearly 60 ultra compact (UC) HII regions lying along the north-to-south elongation (Gaume & Claussen 1990). Bipolar outflows are found from two of the HII complexes, Sgr B2 Main and North (Lis, *et al.* 1993). Also clusters of OH, H_2O and H_2CO masers are found near the HII regions (Mehringer, Goss, & Palmer 1994). Thus Sgr B2 is believed to comprise many clusters of high mass YSOs.

Figure 1 (Left) shows the X-ray image of Sgr B2 in the 2-10 keV band, overlaid on the HII contours. We found more than a dozen X-ray sources, of which the second and third brightest (here, sources No10 and No13) are located in the ultra compact (UC) HII complex Sgr B2 Main. Figure 1 (Right) is the closed-up 2–10 keV band X-ray image near Sgr B2 Main, overlaid on the contours of the UC HII regions F1–F4, G (De Pree, Goss, & Gaume 1998) and I (Gaume & Claussen 1990). The cross (+) indicates the position and 1σ errors ($\sim 1''$) of the MIR source MSX5C G000.6676-00.0355.

No10 seems extended along the UC HII island F3, F4 and G, and would be comprised of several point sources. Thus No 10 may correspond to a cluster of very high mass YSOs (well below 10^5 year). The X-ray spectrum is given in Figure 2 (Left), which is fitted with a thin thermal model as is listed in Table 1.

No13 is also a cluster of X-ray sources lying in the east of the HII region I, but is associated with no UC HII region. This may indicate that No13 is in a pre-phase of UC HII formation, possibly younger than No10. Still it exhibits X-rays with comparable luminosity to No10. Figure 2 (Right) shows the X-ray spectrum, and the best-fit thin thermal mode parameters are listed in Table 1.

The best-fit absorption of 4×10^{23} Hcm^{-2} for No10 and No13 are the largest among any of the X-ray emitting YSOs, indicating that they are lying at/near the center of the core of Sgr B2. This observation also demonstrates that hard X-rays are very powerful to discover deeply embedded stars even if they are suffered with a large optical extinction of $Av \sim 200$-$300\ mag$.

The absorption corrected luminosities in the 2-10 keV band for No10 and No13 are 8×10^{32} ergs s^{-1} and 13×10^{32} ergs s^{-1}, respectively. Since these X-ray sources are likely to be complexes of several YSOs, the luminosity of individual star would be in the order of 10^{32} ergs s^{-1}. This is similar value to the nearest high mass YSO, θ C Ori of spectral type O6-7 (Schulz, *et al.* 2001) and larger than those of high mass young stars in the Monoceros R2 cloud (Kohno, Koyama, & Hamaguchi 2002).

A notable feature of No10 is strong lines at 6.7 keV and 6.4 keV. The former is the K-shell transition line from He-like irons in thin hot plasma. The iron abundance is more than 5 times of solar, which is significantly larger than that from any other high mass star forming regions (SFRs) (Kohno, Koyama, & Hamaguchi 2002, Schulz, *et al.* 2001, Yamauchi *et al.* 1996). The later line (6.4 keV line) may be due to neutral or low-ionization irons in the dense circum/inter

https://doi.org/10.1017/S1743921305004618 Published online by Cambridge University Press

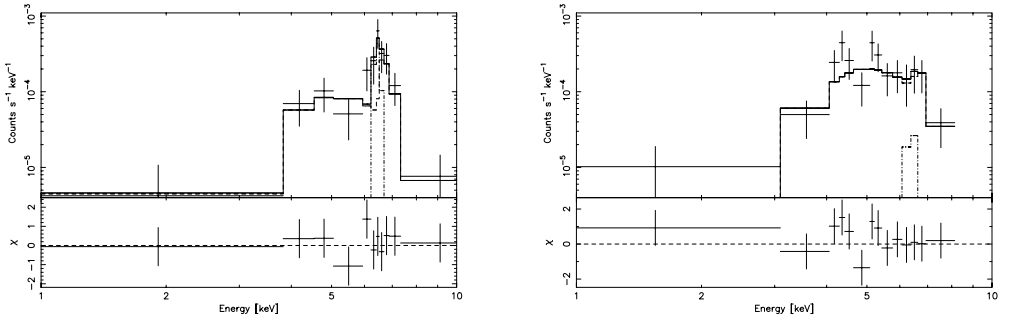

Figure 2. Left: The X-ray spectrum and the best-fit model (solid histogram) of thin thermal plasma with a 6.4 keV line (the dotted histogram) for No10. Right: Same as No 10 (the Left figure) but for No13. [adopted from Takagi, Murakami & Koyama (2002)]

Table 1. X-ray sources in the Sgr B2 Main Complex

Source[1]	kT[2]	$N_{\rm H}$[3]	$L_{\rm x}$[4]	EW[5]
10	10 (4.1-30)	4.0 (1.9-8.8)	8	0.6
13	4.8 ($\geqslant$ 1.1)	4.0 (2.4-7.3)	13	-

Parentheses indicate 90% confidence range.
(1) 10: HII regions F-I, 13: The east of HII region I
(2) Temperature in units of keV
(3) Absorption in units of 10^{23} Hcm^{-2}
(4) Luminosity in the 2-10 keV band in units of 10^{32} ergs s^{-1}
(5) Equivalent width of the 6.4 keV line in units of keV
[adopted from Takagi, Murakami & Koyama (2002)]

stellar medium irradiated by the central stars. The iron abundance of No13, in contrast to No10, is sub-solar.

2.2. *The Arches Cluster*

The Arches Cluster is also a giant molecular cloud located near at the Galactic center(GC). Using the GC survey data, we have resolved at least 3 bright X-ray sources at the position of IR massive stars No21, 23, and 26 (Blum *et al.* 2001). No 23 and No21 are also radio sources AR1 and AR4, hence would have large mass loss of 1.7×10^{-4} and 3.9×10^{-5} $M_\odot$, respectively (Lang, *et al.* 2001).

Figure 3 (Left) is a fine image with the bin size of $0.5''$. The diamond and cross show the position of the bright IR and radio sources, respectively. The best-fit thin thermal model parameters of these sources are listed in Table 2. They show large X-ray absorptions of 10^{23} H cm^{-2}, which is consistent with being cluster members. The X-ray luminosities in the 2-10 keV band of 3-5$\times10^{33}$ ergs s^{-1} are one of the highest among any known YSOs.

There is an elongated diffuse emission with a strong iron line at 6.4 keV. Figure 3 (Right) is the *Chandra* 6.4 keV-line image overlaid on the radio contour. The morphology and spectral feature indicate that the diffuse emission is due to an irradiation by the Arches X-rays with total luminosity of a few$\times10^{35}$ ergs s^{-1} , 10 time larger than the present value. One possibility is that the Arches cluster was brighter X-ray source in the past.

2.3. *The Mon R2 cloud*

Chandra observed the Mon R2 cloud, a high-mass star forming region located at a distance of 830 pc (Racine 1968). From the central $3.2'\times3.2'$ region, we have detected 152 X-ray sources, of which about 85 % are identified to IR sources. To estimate the approximate stellar masses, we

https://doi.org/10.1017/S1743921305004618 Published online by Cambridge University Press

Table 2. High mass YSOs in Arches Cluster

Name	kT^1	$N_{\rm H}^2$	$L_{\rm x}^3$
26	2.4(1.3-5.6)	6.9(4.5-11.2)	2.8(2.3-3.4)
21(AR4)	1.3(0.6-2.5)	9.3(5.6-15.5)	3.9(3.1-4.7)
23(AR1)	1.6(1.0-2.7)	9.9(6.5-14.8)	5.0(4.2-6.0)

Parentheses indicate 90% confidence range.
(1) Thin thermal temperature in units of keV
(2) Absorption in units of 10^{22} Hcm^{-2}
(3) The 2-10 keV band luminosity in units of 10^{33} ergs s^{-1}

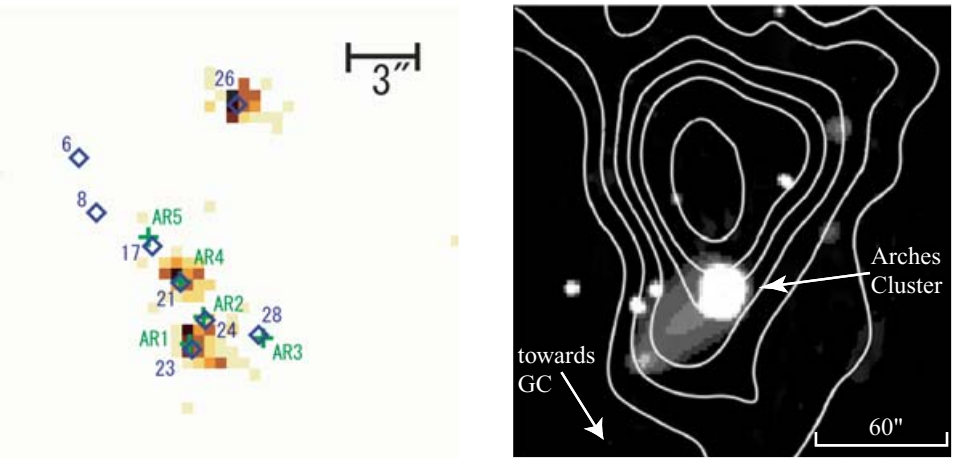

Figure 3. Left: the 2-10 keV band X-ray image of the Arches Cluster. Right: the 6.4 keV band image.

plot in Figure 4 , the $K-mag$ and $H-K$ mag relation and model tracks (solid line) of 2.5 $M_\odot$ star in the ages from 0.07 Myr to 2 Myr (D'Antona, & Mazzitelli 1994). The extinction effect for 2.5 $M_\odot$ stars at the ages of 0.07 Myr and 2 Myr are given by the dashed lines. For the H-band non-detection sources, we assume their H-band magnitude to be 17.6, the completeness limit of Carpenter *et al.* (1997). Open and filled circles represent X-ray detected and non-detected sources, respectively. The radius of the open circles gives logarithmic of the X-ray flux. From Figure 4, we find IRS 1SW, 2, 3SW, 3NE and a_S are well above the 2.5 $M_\odot$ line of any assumed ages.

IRS 1SW has a bolometric luminosity of 3.0×10^3 $L_\odot$ (Henning, *et al.* 1992) and would be a B0 type star in zero age main sequence (ZAMS), which is exciting a compact HII region inside the IR shell (Massi, *et al.* 1985). The X-ray spectrum of IRS 1SW is fitted with a thin thermal plasma model. The best-fit plasma parameters are listed in Table 3.

The IR source a_S has a similar IR spectrum to that of IRS 1SW (Carpenter *et al.* 1997) but has no HII region, hence it would be a similar class to, but is younger than IRS 1SW. The spectrum of a_S is fitted with the best-fit parameters listed in Table 3. These X-ray features are very similar to those of IRS 1SW.

https://doi.org/10.1017/S1743921305004618 Published online by Cambridge University Press

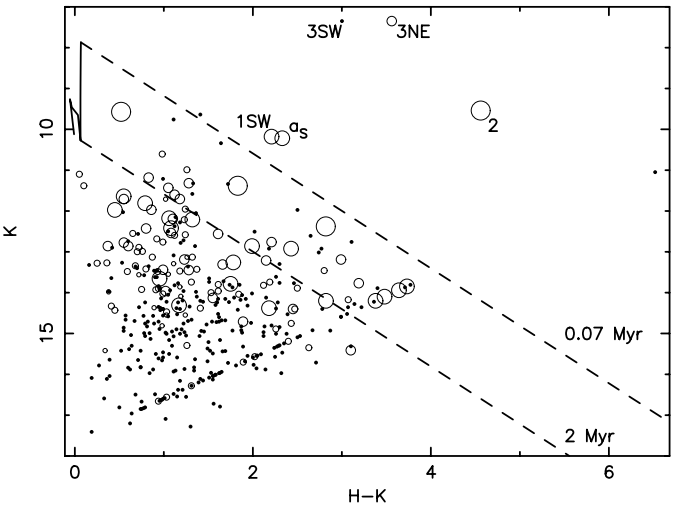

Figure 4. The X-ray flux on the $K - mag$ and $H - K$ mag relation. [adopted from Kohno, Koyama, & Hamaguchi (2002)]

Table 3. High mass YSOs in Mon R2

Name	kT^1	$N_{\rm H}^2$	$L_{\rm x}^3$
IRS 1SW	1.9(1.3-2.8)	4.7(3.5-6.4)	1 (0.6-2.0)
a_S	2.6(1.6-6.2)	6.0(4.0-9.2)	0.6(0.4-1.6)
IRS 2	10.9($\geqslant$ 2.0)	9.1(5.7-17)	0.6(0.5-2.0)

Parentheses indicate 90% confidence range.
(1) Thin thermal temperature in units of keV
(2) Absorption in units of 10^{22} Hcm^{-2}
(3) The 0.5-10 keV band luminosity in units of 10^{31} ergs s^{-1}
[adopted from Kohno, Koyama, & Hamaguchi (2002)]

IRS 2, an illuminating source of the IR shell, has the bolometric luminosity of $6.5 \times 10^3 L_\odot$ (Henning, *et al.* 1992) and would be a cluster of several young embedded sources including BN-like objects, younger stars than ZAMS. The X-ray spectrum of IRS 2 has a thin thermal plasma with the best-fit parameters given in Table 3. The X-ray flux is highly variable with a slow-rise profile at the peak luminosity of 2×10^{31}ergs s^{-1}.

IRS 3, the brightest near- and mid-IR source in Mon R2, has a bolometric luminosity of 1.3×10^4 $L_\odot$, and would be high mass YSOs (Henning, *et al.* 1992). The presence of H_2O and OH masers (Smits, Cohen, & Hutawarakorn 1998) and a compact molecular outflow indicate that IRS 3 is still in a phase of dynamical mass accretion (Giannakopoulou, *et al.* 1997). IRS 3 has been resolved into two sources, IRS 3NE and SW (Carpenter *et al.* 1997). IRS 3NE exhibits heavily absorbed hard X-rays, hence is a candidate of a high mass YSO embedded in the cloud core.

From Table 3, we see that all the high mass young stars in our Mon R2 X-ray samples show a high temperature plasma of ∼2-3 keV. They also exhibit rapid time variability including flare-like events. These are in contrast to high mass main sequence stars (MSSs) which shows lower temperature plasma of $\leqslant$1 keV and relatively stable light curve.

We therefore suspect that high-intermediate YSOs may have magnetic activity rather than stellar wind activity.

The X-ray luminosities of these high mass YSOs in Mon R2 are $\sim 10^{31}$ergs s^{-1}, which are significantly higher than those of low mass YSOs. In order to see the X-ray luminosity as

https://doi.org/10.1017/S1743921305004618 Published online by Cambridge University Press

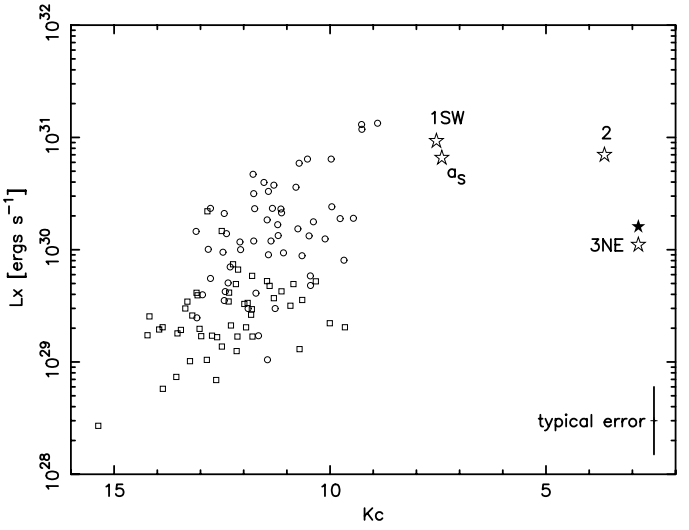

Figure 5. The extinction corrected K-mag ($K_{\rm c}$) and $L_{\rm X}$ relation. [adopted from Kohno, Koyama, & Hamaguchi (2002)]

a function of stellar mass, we plot the relation of extinction corrected K-mag (Kc) and X-ray luminosity ($L_{\rm X}$) in Figure 5. The filled star represents the result of IRS 3NE with a 2-components model. Although the conversion of $K_{\rm c}$ to the stellar mass is not unique, a smaller $K_{\rm c}$ represents a higher mass star, as the first approximation. From Figure 5, we find that $L_{\rm X}$ seems to saturate at $\sim 10^{31}$ ergs s^{-1} in the high mass end.

3. Herbig Ae/Be Stars

Herbig Ae/Be Stars (hereafter, HAeBes) are intermediate mass YSOs. Among the 28 *ASCA* observations on HAeBes, *ASCA* detected 11 plausible X-ray counterparts. One may argue that most of the HAeBes are visible or spectroscopic binaries , whose companion stars could be low-mass YSOs, i.e. T-Tauri Stars (TTSs) or protostars, which are known to emit strong X-rays. We therefore discuss whether or not the HAeBe X-rays observed with *ASCA* come from possible low-mass companions. Since our HAeBe samples have ages of $\sim 10^6$-year, companions stars would be Classical TTSs (CTTSs). Stelzer & Neuhäuser (2001) reports that, in the Taurus Auriga region, CTTSs with log $L_{\rm X} \gtrsim 10^{30}$ ergs s^{-1} are about 5%. All the *ASCA* detected sources have log $L_{\rm X} \gtrsim 10^{30}$ ergs s^{-1} with the detection rate of $\sim$40%. Therefore possibility of low mass companion X-rays could be negligible, at least in our sample.

3.1. *X-ray Temperature and Variability*

The plasma temperatures of our HAeBes are k$T \sim 2$ keV, significantly higher than those of high mass main sequence stars (MSSs). The X-rays of high mass MSSs are due to the stellar wind activity, where the typical velocity of the wind of $v_{\rm wind} \sim 1000$km s^{-1} is shocked and thermalized to a temperature of k$T \sim 1$ keV. We estimate possible temperature using the observed wind velocity in Figure 6 (Nisini *et al.* 1995, Benedettini, *et al.* 1998), where the plasma temperatures of our HAeBe samples are also plotted. We see all the observed X-ray temperature are nearly 10 times larger than that estimated from the stellar wind velocity. We also note that the plasma temperature of $\sim$2 keV is similar to those of low mass YSOs originated from the magnetic activity.

A large fraction of our X-ray samples of HAeBes shows large time variability. In particular, MWC 297 and TY CrA show flare-like events, rapid flux increase and exponential decay. Since the high plasma temperature and these variabilities are similar to those of low mass YSOs, we

https://doi.org/10.1017/S1743921305004618 Published online by Cambridge University Press

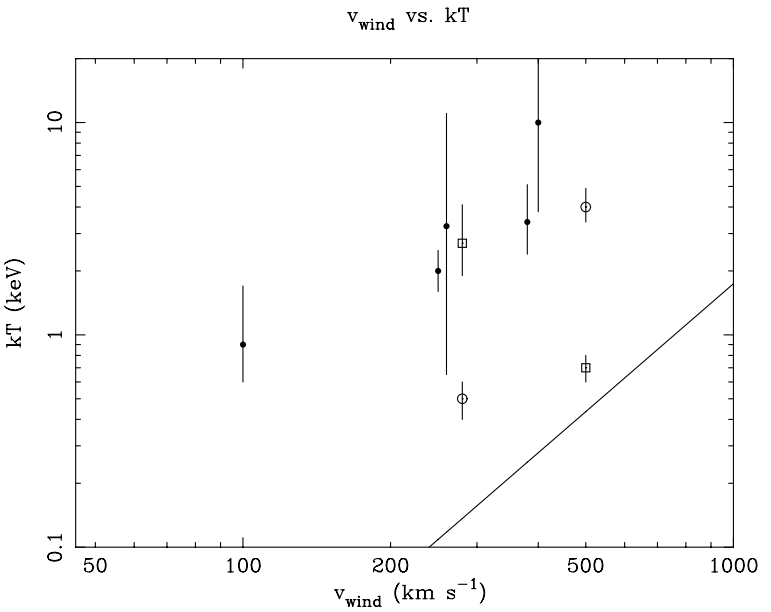

Figure 6. The solid line is estimated relation of HAeBe kT *vs* Wind Velocity. Dots are the results of one-temperature fits, and open circles and squares are those of two-temperature fits. [adopted from Hamaguchi, Yamauchi & Koyama (2005)]

suspect that the X-ray emission from HAeBes is originated from magnetic activity. On the other hand, the $L_{\rm X}/L_{\rm bol}$ ratio is generally smaller than those of low mass YSOs, which means that the magnetic activity is saturated in the high mass region. Furthermore, since the stellar evolutional model of high-intermediate mass YSOs (Palla & Stahler 1990) predicts no surface convection, a key zone of solar type dynamo, different type of magnetic activity may be required.

3.2. *Evolution of Stellar X-ray Activity*

In order to see overall features of X-ray emission of various stars, we plot the X-ray luminosity on the H-R diagram in Figure 7. Sources in the upper right region in the diagram have log $L_{\rm X} \sim 10^{32}$ ergs s^{-1}, and gradually decreases toward the main sequence branch (to the left). In the H-R diagram, we see *X-ray inactive region*, where no source has log $L_{\rm X} > 10^{30}$ ergs s^{-1}. The region is roughly defined as: $3.8 < \log T_{\rm eff}$ (K) < 4.1 and $0.5 < \log L_{\rm bol}/L_{M\odot} < 1.9$, which corresponds to the age older than 10^6 years. We then suggest that the X-ray activity decays with age to below log $L_{\rm X} \sim 10^{30}$ ergs s^{-1} after $\sim 10^6$ years, when the outflow activity terminates (Fuente, *et al.* 1998). We therefore hypothesize that X-ray activity of HAeBe is originated by the reconnection of magnetic fields between star and disk, as suggested for the X-ray origin of low mass protostars by Tsuboi *et al.* (2000) and Montmerle *et al.* (2000).

Finally, we propose a unified scenario for the X-ray activity of stars as follows. X-ray activity in the very early phase is due to fossil magnetic fields from the parent clouds, and the violent activity comes from the magnetic loop reconnection between star and disk (star-disk dynamo). When the disk disappears at $\sim 10^6$ years, the star-disk dynamo has to also disappear. However low mass stars can continue magnetic activity with solar type dynamo even in MSSs, while high mass stars acquire the stellar wind activity. The A - F5 stars of ages $\gtrsim 10^6$ years have neither mechanism, hence fall on the *X-ray inactive region* in the HR diagram.

Acknowledgements

I would like to acknowledge my colleges, Hamauguchi, K., Kohno, Nakajima, Takagi, who provide the *ASCA* and *Chandra* results on high mass young stars. This work is supported by

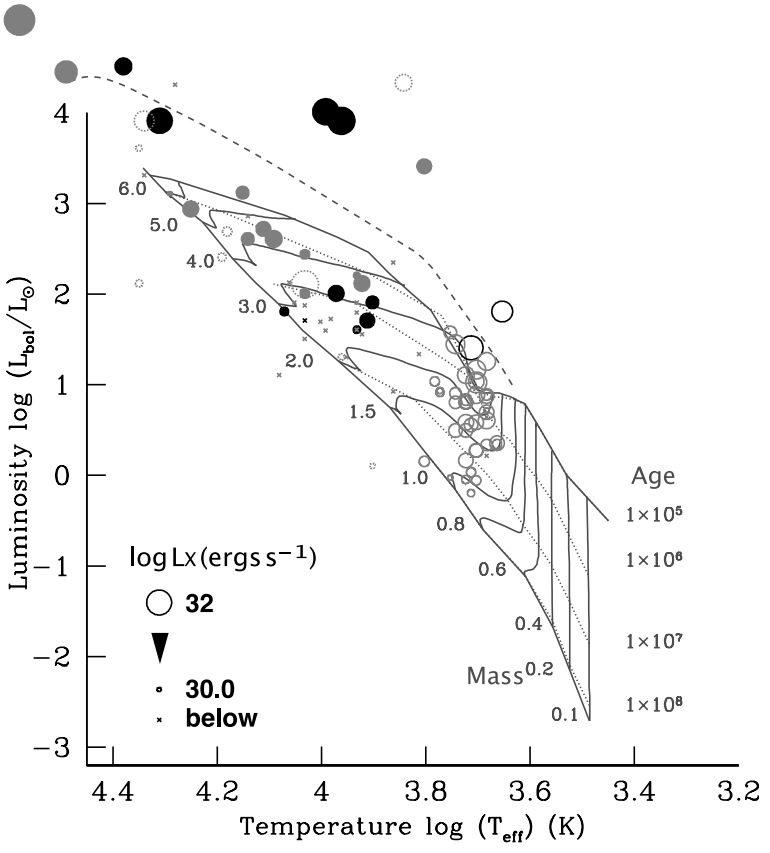

Figure 7. X-ray fluxes plotted on the H-R diagram. Circle size is proportional to (log L_X-30) and Crosses are those of log $L_X < 30$. Luminosity upper limit for log $L_X > 30$ are given by dotted circles. Black and grey represent the *ASCA* and *ROSAR* Samples (Zinnecker & Preibisch 1994). Closed and Open are HAeBes and proto-HAeBe candidate (less massive stars), respectively. The solid tracks are due to the stellar evolution model by Palla & Stahler(1990). [adopted from Hamaguchi, Yamauchi & Koyama (2005)]

the Grant-in-Aid for the 21st Century COE "Center for Diversity and Universality in Physics" from the Ministry of Education, Culture, Sports, Science and Technology (MEXT) of Japan.

References

Benedettini, M., Nisini, B., Giannini, T., Lorenzetti, D.,Tommasi, E., Saraceno, P., & Smith, H. A. 1998, *A&A* 339, 159

Blum, R. D., Schaerer, D., Pasquali, A., Heydari-Malayeri, M., Conti, P. S., Schmutz, W. 2001, *AJ* 122, 1875

Carpenter, J. M., Meyer, M. R., Dougados, C., Strom, S. E., & Hillenbrand, L. A. 1997, *AJ* 114, 198

D'Antona, F., & Mazzitelli, I. 1994, *ApJ* (Supplement) 90, 467

De Pree, C. G., Goss, W. M., & Gaume, R. A. 1998, *ApJ* 500, 847

Fuente , A., Martín-Pintado, J., Rodríguez-Franco, A., & Moriarty-Schieven, G. D. 1998, *A&A* 339, 575

Gaume, R. A. & Claussen, M. J. 1990,*ApJ* 351, 538

https://doi.org/10.1017/S1743921305004618 Published online by Cambridge University Press

Giannakopoulou, J., Mitchell, G. F., Hasegawa, T. I., Matthews, H. E., & Maillard, J. P. 1997, *ApJ* 487, 346
Hamaguchi, K., Yamauchi, S. & Koyama, K. 2005, *ApJ* 618, 360
Henning, Th., Chini, R., & Pfau, W. 1992, *A&A* 263, 285
Kohno, M., Koyama, K., & Hamaguchi, K. 2002, *ApJ* 567. 423; also *Erratum* in *ApJ* 580, 626
Lang, C. C., Goss, W. M., Rodríguez, L. F. 2001, *ApJ* (Letter) 551, L143
Lis, D. C., Goldsmith, P. F., Carlstrom, J. E., & Scoville, N. Z. 1993, *ApJ* (Letter) 402, L238
Massi, M., Felli, M., & Simon, M. 1985, *A&A* 152, 387
Mehringer, D. M., Goss, W. M., & Palmer, P. 1994, *ApJ* 434, 237
Montmerle, T., Grosso, N., Tsuboi, Y., & Koyama, K. 2000, *ApJ* 532, 1097
Nisini, B., Milillo, A., Saraceno, P., & Vitali, F. 1995, *A&A* 302, 169
Palla, F., & Stahler, S. W. 1990, *ApJ* (Letter) 360, L47
Racine, R. 1968, *AJ* 73, 233
Schulz, N. S., Canizares, C., Huenemoerder, D., Kastner, J. H., Taylor, S. C., & Bergtrom, E. J. 2001, *ApJ* 549, 441
Smits, D.P., Cohen, R.J., & Hutawarakorn, B. 1998, *MNRAS*, 296, L11
Stelzer, B., & Neuhäuser, R. 2001, *A&A* 377, 538
Takagi, S., Murakami. H., & Koyama, K. 2002, *ApJ* 573, 275
Tsuboi, Y., Imanishi, K., Koyama, K., Grosso, N., & Montmerle, T. 2000, *ApJ* 532, 1089
Yamauchi, S., Koyama, K., Sakano, M., & Okada, K. 1996, *PASJ* 48, 719
Zinnecker, H., & Preibisch, T. 1994, *A&A* 292, 152